Intracellular chloride channel protein CLIC1 regulates macrophage function through modulation of phagosomal acidification

Lele Jiang[1,*], Kanin Salao[1], Hui Li[1], Joanna M. Rybicka[2], Robin M. Yates[2], Xu Wei Luo[1], Xin Xin Shi[1], Tamara Kuffner[1], Vicky Wang-Wei Tsai[1], Yasmin Husaini[1], Liyun Wu[1], David A. Brown[1], Thomas Grewal[3], Louise J. Brown[4], Paul M. G. Curmi[1,5] and Samuel N. Breit[1,*]

[1]St Vincent's Centre for Applied Medical Research, St Vincent's Hospital and University of New South Wales, Sydney, NSW 2010, Australia
[2]Department of Comparative Biology and Experimental Medicine, Faculty of Veterinary Medicine, and Department of Biochemistry and Molecular Biology, Faculty of Medicine, University of Calgary, Calgary, AB T2N 4N1, Canada
[3]Faculty of Pharmacy, University of Sydney, NSW 2006, Australia
[4]Department of Chemistry and Biomolecular Sciences, Macquarie University, Sydney, NSW 2109, Australia
[5]School of Physics, University of New South Wales, Sydney, NSW 2052, Australia
*Authors for correspondence (l.jiang@amr.org.au; s.breit@amr.org.au)

Accepted 30 July 2012
Journal of Cell Science 125, 5479–5488

doi: 10.1242/jcs.110072

Summary

Intracellular chloride channel protein 1 (CLIC1) is a 241 amino acid protein of the glutathione S transferase fold family with redox- and pH-dependent membrane association and chloride ion channel activity. Whilst CLIC proteins are evolutionarily conserved in Metazoa, indicating an important role, little is known about their biology. CLIC1 was first cloned on the basis of increased expression in activated macrophages. We therefore examined its subcellular localisation in murine peritoneal macrophages by immunofluorescence confocal microscopy. In resting cells, CLIC1 is observed in punctate cytoplasmic structures that do not colocalise with markers for endosomes or secretory vesicles. However, when these macrophages phagocytose serum-opsonised zymosan, CLIC1 translocates onto the phagosomal membrane. Macrophages from CLIC1$^{-/-}$ mice display a defect in phagosome acidification as determined by imaging live cells phagocytosing zymosan tagged with the pH-sensitive fluorophore Oregon Green. This altered phagosomal acidification was not accompanied by a detectable impairment in phagosomal-lysosomal fusion. However, consistent with a defect in acidification, CLIC1$^{-/-}$ macrophages also displayed impaired phagosomal proteolytic capacity and reduced reactive oxygen species production. Further, CLIC1$^{-/-}$ mice were protected from development of serum transfer induced K/BxN arthritis. These data all point to an important role for CLIC1 in regulating macrophage function through its ion channel activity and suggest it is a suitable target for the development of anti-inflammatory drugs.

Key words: Channel, CLIC1, Macrophage, Phagosome, Acidification, Maturation

Introduction

Chloride intracellular channel protein 1 (CLIC1), a member of the highly evolutionarily conserved CLIC family of chloride ion channel proteins, was first cloned because of its increased expression in activated macrophages (Valenzuela et al., 1997). Proteins of the CLIC family are small in size and exist in both soluble cytoplasmic and integral membrane forms, with only a single putative transmembrane region, all features that are unusual for ion channel proteins (Warton et al., 2002). The crystal structure of the soluble monomeric CLIC1 showed that it belongs to the glutathione S-transferase (GST) fold family (Harrop et al., 2001).

Despite these atypical features, the chloride ion channel activity of several CLIC family members has been extensively documented both in transfected cells and using purified recombinant protein added to artificial lipid bilayers (reviewed by Littler et al., 2010). The integral membrane form of CLIC1 is oriented in the plasma membrane with the N-terminus on the exterior and an inward cytoplasmic C-terminus (Tonini et al., 2000). Additionally, the CLIC1 ion channel activity is increased by both oxidative and acidic conditions (Warton et al., 2002; Tulk et al., 2002).

Whilst there is still limited data on the biological role of CLICs, their importance is indicated by their conservation across evolution (Littler et al., 2010). In *C. elegans*, the deletion of one of the two CLIC homologues (EXC-4) causes malformation of the excretory canal suggesting a role in tubulogenesis (Berry et al., 2003). In a somewhat similar process, CLIC4$^{-/-}$ mice display impaired angiogenesis and the formation of collateral vessels (Chalothorn et al., 2009; Ulmasov et al., 2009). In addition, CLIC4$^{-/-}$ mice are protected from endotoxin lipopolysaccharide mortality with reduced serum inflammatory cytokine levels (He et al., 2011). The jitterbug mice, which carry a natural mutation in the *clic5* gene, have impaired hearing and balance (Gagnon et al., 2006). These mice also have proteinuria and are hyperphagic, but are highly resistant to diet-induced obesity (Pierchala et al., 2010; Bradford et al., 2010). Lastly, CLIC1$^{-/-}$ mice we have created are phenotypically normal but have mild platelet dysfunction with

prolonged bleeding time and decreased response to ADP, mediated via the $P2Y_{12}$ receptor (Qiu et al., 2010).

CLIC1 is highly expressed in macrophages, which are key cells in innate and adaptive immunity. As such, they play crucial roles in tissue homeostasis, wound repair and host defence. In chronic inflammatory diseases, they are a major source of pro-inflammatory molecules. Macrophages ingest pathogens, foreign particulates, or apoptotic cells by phagocytosis to form phagosomes. During the course of phagocytosis, phagosomes mature progressively by fusion with acidic early and late endosomes, as well as lysosomes, resulting in progressive phagosomal acidification (Vieira et al., 2002; Russell et al., 2009). The process of phagosome maturation is in part dependent on Rho GTPases and the scaffold proteins ezrin-radixin-moesin (ERM), both of which are regulators of the reorganisation of the actin cytoskeleton (Erwig et al., 2006).

Whilst the phagosome's acquisition of constituents from the fusion with endosomes plays a key role in its acidification, phagosomal membrane ion channels and transporters are also important. The vacuolar-type H^+-ATPase (v-ATPase) is a proton pump distributed to various exocytic and endocytic vesicles and is recruited to the phagosomes from lysosomes during phagosomal maturation (Sun-Wada et al., 2009), where it plays an important role in phagosomal acidification (Lukacs et al., 1990), perhaps by providing a net positive charge of the phagosomal lumen (Lamb et al., 2009). A voltage-gated proton channel is also found on phagosomal membranes (Okochi et al., 2009) and both v-ATPase and the proton channel are thought to compensate the charge generated by the activation of NADPH (nicotinamide adenine dinucleotide phosphate) oxidase (Rybicka et al., 2011), during the respiratory burst.

NADPH oxidase is the reactive oxygen species (ROS) generating oxidase activated during the respiratory burst in response to pathogen invasion. In the resting state it is composed of the integral membrane subunits gp91phox and p22phox and the soluble, cytosolic subunits p67phox, p47phox, p40phox and Rac2, a Rho GTPase. Upon activation the soluble subunits of the NADPH oxidase complex are recruited to phagosomal membranes where they bind gp91phox resulting in the transfer of electrons across the wall of the phagocytic vacuole and the generation of superoxide in the lumen (Segal and Shatwell, 1997). The passage of electrons across the membrane results in a negatively charged lumen (Lamb et al., 2009), which is compensated by the influx of protons via the v-ATPase and the voltage-gated proton channel (Liu and Chu, 2006; DeCoursey, 2010).

Chloride ion channels and transporters are also important in regulating the phagosomal environment through counter ion regulation and charge compensation (Scott and Gruenberg, 2011). During phagosomal-endosomal acidification an influx of Cl^- occurs through ion channels and transporters like members of the ClC family (Lamb et al., 2009) and the cystic fibrosis transmembrane-conductance regulator (CFTR; Di et al., 2006; Deriy et al., 2009). For example, both early and late endosomes from ClC-3 null hepatocytes display decreased acidification and chloride ion concentration (Hara-Chikuma et al., 2005). However, it is not clear exactly how the chloride ion channels and transporters are regulated in relation to phagosomal maturation. Whilst some (Di et al., 2006; Deriy et al., 2009) have reported that deletion of CFTR in murine alveolar macrophages, but not peritoneal macrophages, caused substantial impairment of phagosomal acidification, others (Haggie and Verkman, 2007; Barriere et al., 2009) found no correlation between CFTR activity and phagosomal/lysosomal acidification in either macrophages or epithelial cells. More recently it was found that neither the deletion of CFTR nor ClC-7 from the RAW264.7 and J774 macrophages resulted in abnormal lysosomal acidification (Steinberg et al., 2010).

Since CLIC1 is an intracellular chloride ion channel protein highly expressed in macrophages, we sought to investigate its role in macrophage phagosome function. In this study, we show that in resting macrophages, CLIC1 is widely distributed in the cytoplasm in a punctate pattern. Shortly after initiation of phagocytosis CLIC1 appears on phagosomal membranes where it can be seen along with ERM proteins, the Rho GTPases, Rac2 and RhoA, and NADPH oxidase components. Comparison between macrophages from $CLIC1^{+/+}$ and $CLIC1^{-/-}$ mice show that $CLIC1^{-/-}$ macrophages have an elevated phagosomal pH. We then demonstrate that several consequences on phagosomal function from an elevated pH include decreased phagosomal proteolytic activity and reduced ROS production. Consistent with this, $CLIC1^{-/-}$ mice are protected from the development of a macrophage-dependent immune-complex mediated arthritis.

Results

Subcellular localisation of CLIC1 in peritoneal macrophage

To help decipher the role of CLIC1 in macrophage function, we first employed immunofluorescence confocal microscopy to determine its subcellular localisation. In the resting peritoneal macrophage, CLIC1 staining was punctate and denser toward the centre of the cells in the perinuclear region (Fig. 1). No staining was present in $CLIC1^{-/-}$ cells (data not shown).

In order to try to determine whether the punctate CLIC1 staining was on early endosomes, we first examined the spatial correlation between CLIC1 and EEA1 (Fig. 1A-D). Whilst both are distributed throughout the cytoplasm and are at higher density in the perinuclear area, CLIC1 and EEA1 do not co-localise as can be seen in areas towards the periphery of the cell, where the staining is not overly dense (Fig. 1C,D). Similarly CLIC1 staining does not colocalise with transferrin-positive endosomes (Fig. 1E-H) or a number of other vesicular markers including LBPA (late endosome), LAMP1 (lysosome), rab11 (recycling endosome), calnexin (endoplasmic reticulum; ER), and PM130 (Golgi) (data not shown). These data indicate that in resting macrophages, the punctate CLIC1 staining is not associated with typical endosomes, lysosomes, ER or Golgi apparatus. However, it is possible that the CLIC1-containing structures are vesicles which lack typical endosomal markers. In addition, as CLIC1 has no signal peptide it would be synthesised on cytoplasmic ribosomes which also display a punctate staining pattern.

CLIC1 is present on phagosomal membranes

In order to determine whether CLIC1 translocates to phagosomal membranes, we stained peritoneal macrophages 5 minutes after they had undergone synchronised phagocytosis of serum-opsonised zymosan (Fig. 2). The zymosan containing phagosomes are clearly identifiable by their quasi-circular cross section and well-defined void. As EEA1 is a known membrane protein, the spatial correlation of CLIC1 and EEA1 indicates both proteins are in or on the phagosomal membrane at this time point (Fig. 2A,B, arrows). Consistent with an early point in phagosome maturation,

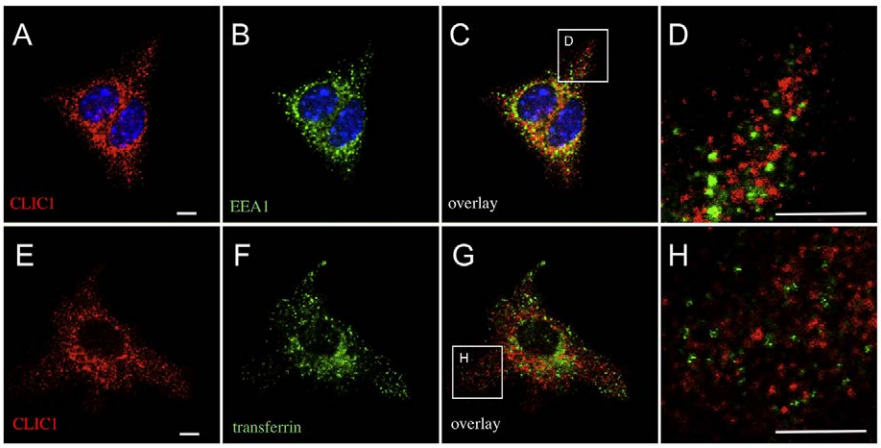

Fig. 1. Subcellular localisation of CLIC1 in resting macrophage. Immunofluorescence confocal microscopic images show a resting peritoneal macrophage from CLIC1$^{+/+}$ mice (**A–D**) stained with the CLIC1 antibody (A,C,D, red) which does not colocalise with EEA1 positive early endosomes (B,C,D, green). The nuclei have been stained (blue) using TO-Pro 3 (A–C). (**E–H**) The CLIC1 punctate structure (E,G,H, red) does not colocalise with transferrin positive endosomes (F,G,H, green). Scale bar: 5 μm.

at 5 minutes after phagocytosis, LAMP1 staining appears in sections of some phagosomal membranes (Fig. 2E), but there is minimal overlap with CLIC1 (Fig. 2F).

It should be noted that the morphology of the macrophages in the Fig. 2 appears somewhat different compared to that in the Fig. 1 is due to the difference in the focal plains for confocal microscopy. Fig. 1 is of a resting macrophage and the imaging focal plane is close to the glass slide where many distinguishable 'punctate' CLIC1 structures can be seen. Following addition of opsonised zymosan, the cells become activated and change shape. Further the zymosan particles are about 3-5 μm in diameter which also define the size of phagosomes. Thus in order to display the most representative view for phagosomes, the focal plane is a few microns above the glass slide (Fig. 2).

Spatial correlation of CLIC1 with ERM, Rac2, and RhoA on phagosomal membranes

Phagosome maturation requires significant cytoskeleton reorganisation which is regulated by the scaffold proteins ERM, and small GTPases such as Rac2 and RhoA which localise to the phagosomal membrane during this process (Erwig, et al., 2006; Marion, et al., 2011). We therefore next asked whether CLIC1 was localised in proximity to these cytoskeletal or membrane proteins that regulate phagosomal maturation (Fig. 3). At 5 minutes after synchronised phagocytosis, CLIC1 can be seen on the phagosomal membrane as well as ERM proteins (Fig. 3A-C), Rac2 (Fig. 3D-F) and RhoA (Fig. 3G-I). Consistent with the cellular distribution of ERM proteins, in addition to the phagosomal membrane, ERM proteins are also seen along pseudopodia (Fig. 3B,C). These markers are also examined on the CLIC1$^{-/-}$ macrophages after 5 min synchronised phagocytosis and their presence on phagosomal membranes is not detectably altered (data not shown).

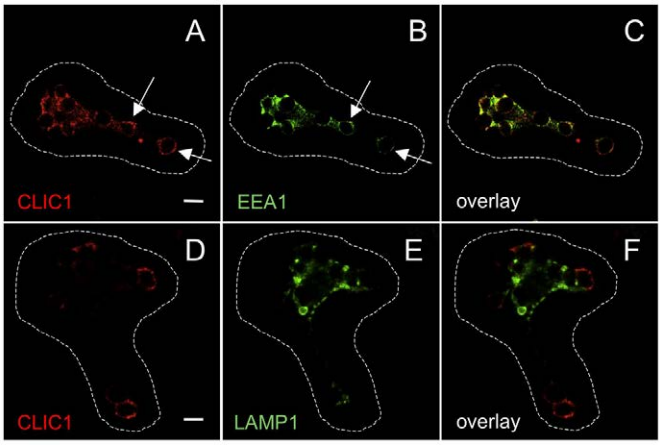

Fig. 2. CLIC1 is localised to the phagosome membrane. Confocal fluorescence microscopy of peritoneal macrophages 5 min after phagocytosis of serum-opsonised zymosan particles. Cells were stained with antibody to CLIC1 (**A**,**C**,**D**,**F**, red), and the membrane markers EEA1 (**B**,C, green) or LAMP1 (**E**,F, green). Scale bar: 5 μm.

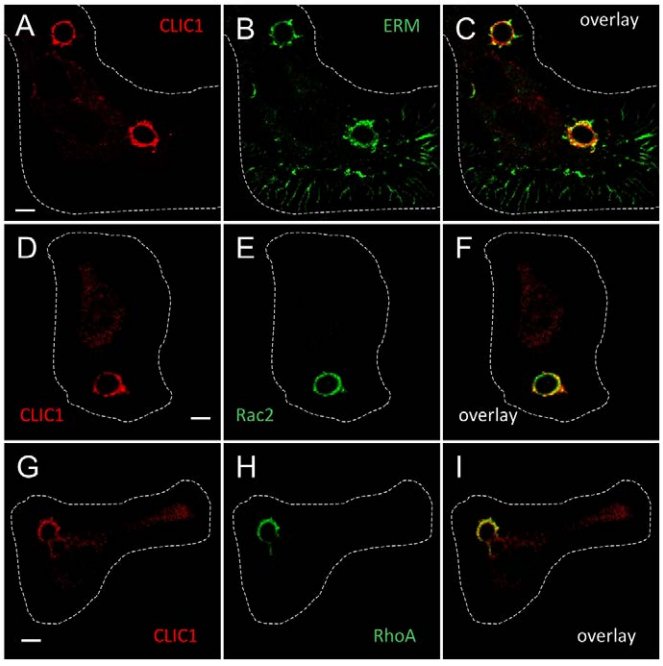

Fig. 3. Spatial correlation of phagosome localised CLIC1 with ERM, Rac2, and RhoA. Confocal fluorescent microscopy of peritoneal macrophages, 5 min after phagocytosis of serum-opsonised zymosan particles, were stained for CLIC1 (**A**,**C**,**D**,**F**,**G**,**I**, red) and either ERM (**B**,**C**, green), Rac2 (**E**,F, green) or RhoA (**H**,**I**, green). Scale bar: 5 μm.

Spatial correlation of CLIC1 and NADPH oxidase components on the phagosomal membranes

As shown above, on phagosomal membranes of activated macrophages, CLIC1 colocalises with Rac2, a small GTPase, which can form part of the NADPH oxidase complex (Fig. 3D-F). NADPH oxidase is a phagocytic ROS generating enzyme complex present on the macrophage phagosomal membrane. We next examined the spatial relationship between CLIC1 and the other two NADPH oxidase components in macrophages that had phagocytosed serum-opsonised zymosan. As expected, both gp91phox (Fig. 4A-C), the membrane integrated subunit, and p67phox, the soluble subunit that forms a membrane-bound complex with gp91phox on activation (Fig. 4D-F) are present on phagosomal membrane although CLIC1 and the integrated membrane gp91phox clearly had distinct distribution patterns (C, arrow). The presence of NADPH oxidase components on the phagosomal membrane of CLIC1$^{-/-}$ macrophages does not show detectable difference when compared to CLIC1$^{+/+}$ macrophages (data not shown).

Phagosomes from CLIC1$^{-/-}$ macrophages display impaired acidification

The localisation of the CLIC1 chloride ion channel protein to phagosomal membranes suggests that it may participate in the regulation of phagosomal pH. We therefore monitored the process of phagosomal acidification by live cell imaging of peritoneal macrophages that had phagocytosed serum-opsonised zymosan particles labelled with either FITC or Oregon Green 488. These two probes were used as FITC can effectively differentiate pHs between 5.5 and 7.5 and Oregon Green between 3.5 and 5.5 (supplementary material Fig. S2).

Following synchronised phagocytosis, the phagosomes rapidly acidified. Over the first 4 minutes, phagosomal pH dropped from near neutral to below 5.5 in both CLIC1$^{+/+}$ and CLIC1$^{-/-}$ macrophages with no distinguishable difference between the two (Fig. 5A). From 4-7 min, the phagosomal pH dropped by ~0.5 pH units with the acidification of CLIC1$^{-/-}$ cells clearly less than CLIC1$^{+/+}$ cells for time points beyond 6 min (Fig. 5A). In both CLIC1$^{+/+}$ and CLIC1$^{-/-}$ macrophage phagosomes, the rate of acidification slowed from 8 min onwards and reached a steady state at about 20-30 min at which point the average phagosomal pH (Fig. 5B) of CLIC1$^{-/-}$ macrophages (4.13 ± 0.02, $n=7$ animals and >10 zymosan containing phagosomes analysed per animal) was about 0.2 units higher than that of the CLIC1$^{+/+}$ (3.92 ± 0.03, $n=7$ animals and >10 zymosan containing phagosomes analysed per animal, $P<0.001$, unpaired two tailed *t*-test). CLIC1$^{-/-}$ macrophages clearly exhibit an impaired capacity to acidify phagosomes.

The CLIC1 ion channel blocker IAA94 raises the pH of CLIC1$^{+/+}$ phagosomes

IAA94 blocks the ion channel activity of CLIC1 and other CLIC family ion channel proteins (Landry et al., 1989; Tulk et al., 2000; Warton et al., 2002). IAA94 treatment of CLIC1$^{-/-}$ macrophages had no effect on phagosomal pH (4.14 ± 0.01, $n=3$ animals and >10 zymosan containing phagosomes analysed per animal, $P=0.79$); but treatment of CLIC1$^{+/+}$ macrophages significantly raised their phagosomal pH from 3.92 ± 0.03 to pH 4.17 ± 0.05 ($n=4$ animals and >10 zymosan containing phagosomes analysed per animal, $P<0.001$ unpaired two tailed *t*-test) (Fig. 5B). The latter was not significantly different to that of CLIC1$^{-/-}$ macrophages. This provides further support for the role of CLIC1 on phagosomal acidification. The fact that IAA94 did not further impair phagosomal acidification in CLIC1$^{-/-}$ macrophages, as it did in CLIC1$^{+/+}$ macrophages indicates the effect is CLIC1 specific and does not involve the compensatory contribution of other CLICs. Further it also indicates that IAA94 does not have any off-target effects in this system.

Deficient ROS production does not alter macrophage phagosomal pH

As CLIC1 chloride channel activity may be influenced by redox, we wished to determine whether CLIC1 dependent phagosomal acidification is also dependent on NADPH oxidase activity. We therefore examined the phagosomal pH of macrophages from gp91phox$^{-/-}$ mice which lack NADPH oxidase activity. Using live cell imaging as above, we found the deletion of gp91phox does not alter the kinetics of the acidification curve (data not shown) nor the steady state phagosomal pH (3.91 ± 0.01; $n=3$ animals and >10 zymosan containing phagosomes analysed per animal, $P=0.96$) (Fig. 5B). This is consistent with previously published data (Rybicka et al., 2010) and indicates that activation of the NADPH oxidase complex and consequent ROS production does not influence macrophage phagosomal pH.

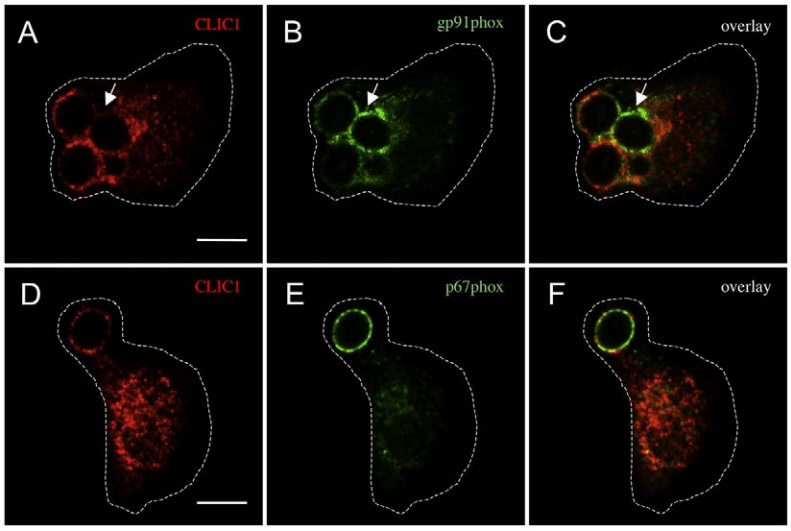

Fig. 4. Spatial correlation of CLIC1 with NOX2 components. Confocal fluorescent microscopy of peritoneal macrophages 5 min after phagocytosis of serum-opsonised zymosan particles were stained for CLIC1 (A,C,D,F, red) and either gp91phox (B,C, green) or p67phox (E,F, green). CLIC1 and both gp91phox and p67phox appear on the phagosomal membrane although CLIC1 and gp91phox have different distribution patterns (arrows, A–C). Scale bar: 5 µm.

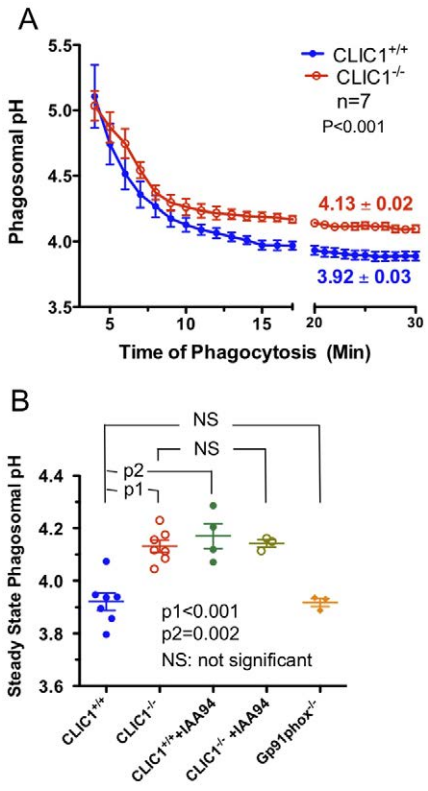

Fig. 5. Phagosomal acidification. Intraphagosomal pH of peritoneal macrophages that had undergone synchronised phagocytosis of serum-opsonised zymosan particles covalently coupled with the pH-sensitive fluorescence probe Oregon Green, were monitored by live cell imaging on an inverted Zeiss Axiovert 200 M microscope with excitation at 490 nm and emission at 525 nm. Zymosan containing macrophage phagosomes from 7 pairs of CLIC1$^{+/+}$ and CLIC1$^{-/-}$ mice were followed in real time and the pH calculated at 60 second intervals (**A**). The steady state pH, calculated as the average pH between 20 and 30 minutes after synchronised phagocytosis, is displayed for CLIC1$^{+/+}$ and CLIC1$^{-/-}$ macrophage phagosomes, with or without the CLIC ion channel blocker IAA94 (**B**). Steady state phagosomal pH from peritoneal macrophages from gp91phox$^{-/-}$ mice is also displayed (B).

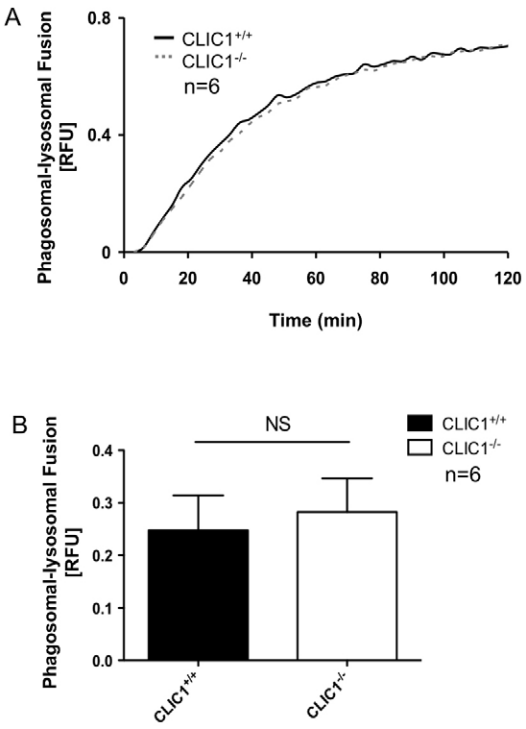

Fig. 6. Phagosomal-lysosomal fusion. Absence of CLIC1 channel does not affect phagosomal-lysosomal fusion in macrophages. Phagosomal-lysosomal fusion was measured by recording FRET efficiency between a particle-bound donor fluorophore Alexa Fluor 488 (excitation 485 nm; emmision 520 nm) and a fluid-phase lysosomal acceptor fluorophore Alexa Fluor 594 hydrazide (excitation 485 nm; emmision 620 nm) relative to the donor fluorescence. Relative fluorescent units (RFU) indicate the concentration of lysosomal constituents within the phagosome at any given point in time. Error bars denote SEM. No statistically significant differences were found between samples using Student's *t*-test. The data are representative of six independent experiments. (**A**) Representative real-time trace. (**B**) Average rate of the FRET efficiency acquisition over six independent experiments. Rates were determined by calculation of the slope of the linear portion of the real-time traces (as described by y=mx+c, where y is relative fluorescence, m is the slope and x is time).

Deficient CLIC1$^{-/-}$ phagosomal acidification is not due to a decrease in phagosomal-lysosomal fusion

Time-dependent fusion between lysosomes and the maturing phagosome is an important mechanism mediating phagosomal acidification. Since we have observed that CLIC1$^{-/-}$ macrophages displayed a decreased capacity to acidify their phagosomal lumen, we wanted to know whether this change may be caused by or have an impact on the rates or extents of phagosomal-lysosomal fusion. To this end we performed a real-time assay that utilises the Förster resonance energy transfer (FRET) principle to measure the signal between an acceptor fluorophore that has been chased into lysosomes and a donor fluorophore restricted to an IgG-opsonised bead (Yates et al., 2005; Yates and Russell, 2008). The FRET fusion profiles generated in CLIC1$^{+/+}$ and CLIC1$^{-/-}$ macrophages (Fig. 6) demonstrate that the absence of CLIC1 does not influence the phagosomal-lysosomal fusion process in macrophages.

Small pH differences modulate *in vitro* proteolysis

Whilst CLIC1$^{-/-}$ mice have a clear defect in macrophage phagosomal acidification, the pH difference between CLIC1$^{-/-}$ and CLIC1$^{+/+}$ mice is small, raising the question as to whether this pH difference is sufficient to alter phagosomal functions. In order to determine if alteration in phagosome pH, of as little as 0.2 units, will result in significant alteration of protein degradation, we first used an *in vitro* model of phagosome proteolysis using BSA in buffers that mimic the acidic phagosomal conditions. Isolated microsomes from the murine brain macrophage (microglial) cell line BV2, were incubated with BSA at a range of different pH values between 4.0 and 4.6. SDS-PAGE with Coomassie Blue staining was used to monitor the degradation patterns of BSA. Each increment of 0.2 units substantially altered the pattern of BSA proteolysis (Fig. 7A). Thus, over the pH range in question, pH differences as small as 0.2 pH units are able to alter the rate and pattern of protein degradation by acidic proteases associated with microglial microsomes.

CLIC1$^{-/-}$ macrophages display impaired phagosomal proteolysis

To directly examine whether reduced phagosomal acidification in CLIC1$^{-/-}$ macrophages alters phagosomal proteolysis, we used live cell imaging to monitor cells that had engulfed 3 μm silica

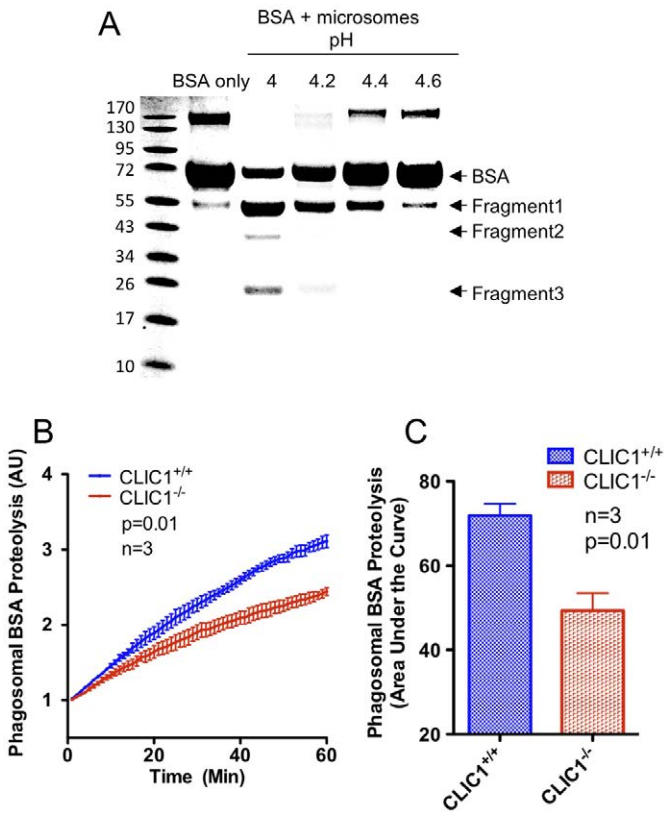

Fig. 7. CLIC1$^{-/-}$ macrophages display a reduced proteolysis. BSA (100 μg) was incubated with isolated microsomes (20 μl) from BV2 cells for 30 min at 37℃ in a buffer with pH calibrated to either 4, 4.2, 4.4 or 4.6, respectively. The BSA degradation pattern was demonstrated by SDS-PAGE and Coomassie Blue staining of the whole gel (**A**). Phagosomal proteolysis of BSA was monitored in real time by live cell imaging of individual phagosomes from peritoneal macrophages that had undergone synchronised phagocytosis of 3 μm silica beads covalently coupled with DQ-bodipy BSA and Alexa Fluor-594 on an inverted Zeiss Axiovert 200 M microscope. Fluorescence signals were acquired from both the DQ-bodipy BSA (excitation 490 nm, emission 525 nm) and Alexa Fluor 594 (excitation 570 nm, emission 620 nm) and used for ratiometric calculation of proteolysis, which appears as an increase in fluorescence (**B**). The total BSA proteolysis measured as the area under the curve is significantly lower in CLIC1$^{-/-}$ macrophages than that of CLIC1$^{+/+}$ (**C**).

beads. These beads were coupled to Alexa Fluor 594 as a reference dye and DQ bodipy BSA, which becomes more fluorescent as its self-quenching is reduced by BSA proteolysis (Seetoo et al., 1997). Isolated peritoneal macrophages from 3 pairs of CLIC1$^{+/+}$ and CLIC1$^{-/-}$ mice, underwent synchronised phagocytosis of the labelled beads which were then monitored by live cell imaging. Change in fluorescence was recorded for 60 min and BSA proteolysis was determined by the gain in fluorescence intensity (Fig. 7B). Proteolysis of BSA was calculated as the area under curve generated by data from at least 30 bead containing phagosomes per animal (Fig. 7C). For CLIC1$^{+/+}$ macrophages this was 71.9±2.8 U, which was significantly more than for CLIC1$^{-/-}$ cells (49.4±4.1 U, n=3, P<0.01). As fluorescence increase is correlated to BSA degradation, this clearly indicates that CLIC1$^{-/-}$ macrophages have much less efficient phagosomal proteolytic capacity.

CLIC1$^{-/-}$ macrophages have attenuated ROS production

The data above clearly depicts macrophage dysfunction in CLIC1$^{-/-}$ mice, which correlates with impaired acidification during phagosomal maturation. Another pH sensitive phagosomal function is NADPH oxidase mediated ROS production. We monitored ROS production using real time measurement of HRP-enhanced luminol chemiluminescence in 96 well plates containing ~50,000 isolated CLIC1$^{-/-}$ or CLIC1$^{+/+}$ peritoneal macrophages per well. The cells in the reaction mix were first monitored for the background chemiluminescence for 10 min before addition of serum-opsonised zymosan (50 μg/ml) and the gain in chemiluminescence intensity with the production of ROS were recorded over the next 60 min (Fig. 8A). Calculated as the area under the curve, CLIC1$^{-/-}$ produced about 30% less ROS (85.7±5.2×10^3 U, n=5) than CLIC1$^{+/+}$ cells (123.7±10.7×10^3 U, n=5, P=0.0127) (Fig. 7B). Further, the CLIC ion channel blocker IAA94 reduced the ROS production from CLIC1$^{+/+}$ macrophage so that it was not significantly different to that of CLIC1$^{-/-}$ macrophage (67.5±5.6×10^3 U, n=5, for CLIC1$^{+/+}$; and 60.8±7.6×10^3 U, n=5, for CLIC1$^{-/-}$; P=0.498). As expected, the NADPH oxidase inhibitor DPI abolished the ROS production

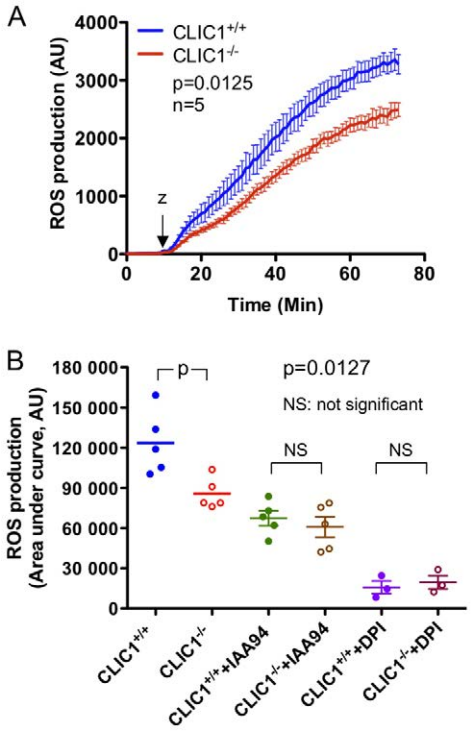

Fig. 8. Reactive oxygen species production. ROS production from peritoneal macrophages from five pairs of CLIC1$^{+/+}$ and CLIC1$^{-/-}$ mice initiated by phagocytosis of serum-opsonised zymosan particles, measured by horse radish peroxidase enhanced luminol chemiluminescence, was monitored in real time on a FLUOstar OPTIMA microplate reader. At the conclusion of the experiment, cell number determination was performed on each well of the 96 well plate to normalise the chemiluminescence signal (**A**). The total ROS production measured as the area under the curve is significantly lower in CLIC1$^{-/-}$ macrophages than that of CLIC1$^{+/+}$ (**B**). The chloride channel blocker IAA94 eliminated any significant difference in ROS production between CLIC1$^{+/+}$ and CLIC1$^{-/-}$ macrophages treated as in A. The NADPH oxidase inhibitor DPI, abolished the ROS production from CLIC1$^{+/+}$ and CLIC1$^{-/-}$ macrophages (B).

from both CLIC1$^{+/+}$ and CLIC1$^{-/-}$ (Fig. 8B). This data further supports the presence of broad based alteration of *in vitro* function of peritoneal macrophages from CLIC1$^{-/-}$ mice.

CLIC1$^{-/-}$ mice are protected from K/BxN arthritis

As phagosomal proteases and ROS are important mediators of tissue injury in acute and chronic inflammatory responses, we examined the effect of CLIC1 gene deletion on the K/BxN serum transfer model of arthritis (Ditzel, 2004), which is macrophage dependent (Solomon et al., 2005). Following a single intraperitoneal injection of K/BxN serum CLIC1$^{+/+}$ mice almost immediately developed an inflammatory arthritis which reached maximum on day 14 with an average of swelling index of 117±2.6% (n=6) (Fig. 9). The swelling then started to resolve and almost reduce to the baseline level on day 28 when the study was terminated. The CLIC1$^{-/-}$ mice, on the other hand, were protected from the arthritis with minimal if any swelling throughout the entire course of observation with a swelling index of 104±2.3% on day 14 (n=6, P<0.01, unpaired two tailed t-test).

Discussion

In this study, we demonstrate that in resting macrophages, CLIC1 is localised to unidentified punctate cytoplasmic structures (Fig. 1) and after ingestion of serum-opsonised zymosan, it moves to the phagosomal membrane (Fig. 2). At least one role of phagosome localised CLIC1 is to help acidify the phagosome as CLIC1$^{-/-}$ macrophages consistently display a phagosomal pH that is 0.2 units higher than CLIC1$^{+/+}$ cells (Fig. 5). To start to explore the mechanisms underlying CLIC1 effect in phagosomal acidification, we first examined whether the CLIC1 chloride channel activity is responsible by using the chloride channel blocker IAA94. The blockade of CLIC1 by IAA94 eliminated any significant pH difference between CLIC1$^{-/-}$ and CLIC1$^{+/+}$ macrophage phagosomes (Fig. 5). IAA94 is a small and highly hydrophobic molecule that binds CLIC proteins with high affinity (Landry et al., 1989). Whilst its mechanism of action is not well characterised limited data indicates that IAA94 binds to the ion channel pore of CLIC family proteins (Singh et al., 1991). The simplest interpretation of these results is that the abrogation of the CLIC1 ion channel activity is responsible for the reduced phagosome acidification in macrophages from CLIC1$^{-/-}$ mice.

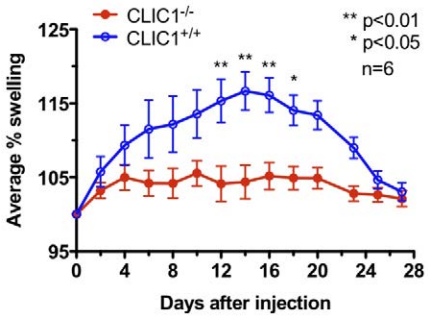

Fig. 9. CLIC1$^{-/-}$ mice are protected from K/BxN serum transfer arthritis. CLIC1$^{-/-}$ and sex matched CLIC1$^{+/+}$ mice aged 8-12 weeks, were injected intraperitoneally with a single dose of 300 µl K/BxN serum. The development of arthritis was assessed using a swelling index generated from the thickness of footpads and ankles measured over 28 days using a calliper before the injection (baseline) and then once every other day. The swelling index is calculated as: (thickness/baseline)×100.

As IAA94 acts on all CLIC proteins and did not further reduce pH in CLIC1$^{-/-}$ mice, it is unlikely that other CLICs are involved in this process.

Apart from ion regulation, an alternative mechanism for phagosomal acidification lies in phagosome maturation resulting from step-wise fusion between phagosomes and endosomes/lysosomes. For this reason we have examined whether CLIC1 participates in phagosomal-lysosomal fusion using a sensitive FRET based assay (Fig. 6). Our findings clearly indicate that CLIC1 does not modulate fusion between the phagosome and lysosomes. Therefore, phagosomal acidification by CLIC1 is likely to be mediated by its chloride ion channel activity rather than by altering phagosomal-lysosomal fusion.

There are several unanswered questions about the role of CLIC1 in phagosomes. Firstly, it is unclear how CLIC1 is incorporated into the phagosomal membrane. Our data (Fig. 1) show that CLIC1 normally resides in the 'punctate' intracellular structures but not typical early or late endosomes. This may be consistent with the fact that CLIC1 is transcribed from RNA lacking a leader sequence for membrane insertion, and therefore does not follow conventional secretory pathway through rough ER and Golgi apparatus (Valenzuela et al., 1997). However, it is yet to be determined whether CLIC1 is incorporated into the endosomal membrane before its subsequent presence in the phagosomal membrane, or CLIC1 inserts into the phagosomal membrane directly from cytosolic CLIC1, and whether the CLIC1 membrane incorporation requires synergistic actions of other proteins, e.g. small GTPases, or ERM proteins.

Irrespective of the mechanism by which CLIC1 modulates phagosomal pH, impaired phagosome acidification is capable of causing profound alterations on macrophage function. A change of 0.2 pH units substantially impairs protein degradation (Fig. 7) and ROS generation (Fig. 8), but may also modulate other phagosomal functions, such as the killing and degradation of engulfed microorganisms, antigen processing and presentation to T lymphocytes and the course of chronic inflammatory processes. Consistent with these *in vitro* actions, we have demonstrated that the CLIC1$^{-/-}$ mice are protected from developing chronic joint inflammation in the K/BxN model of immune complex arthritis (Fig. 9).

K/BxN serum transfer arthritis is initiated by passive transfer of serum containing anti-glucose-6-phosphate isomerase autoantibody. This antibody forms immune complexes in mouse joints, which are endocytosed to initiate an inflammatory response. Because of the mechanism of initiation, this form of arthritis is dependent on the innate immune and inflammatory responses and is largely independent of adaptive immunity. Thus key to the pathogenesis of this arthritis are leukocytes like neutrophils, mast cells and macrophages and their major pro-inflammatory products such as IL-1β and TNFα (Kannan et al., 2005). Directly relevant to this paper, mice depleted of macrophages were completely resistant to the K/BxN arthritis (Solomon et al., 2005). Thus whilst the precise mechanism by which CLIC1 deletion protects mice from K/BxN inflammatory arthritis is unclear, the fact that CLIC1 acts on a key macrophage pathways suggests this is likely to be directly or at least in part responsible. Further, the fact that consistent effects occur *in vivo* adds significantly to the weight of the *in vitro* observations.

In conclusion, our data provides strong evidence that CLIC1 is localised to phagosomal membranes where it regulates phagosomal acidification and consequently, other phagosomal

functions such as proteolysis and ROS production. These *in vitro* changes are reflected *in vivo* in CLIC1$^{-/-}$ mice which are protected from at least one animal model of a chronic inflammatory disease. CLIC1 may thus be a useful target for the development of therapy for this important group of diseases.

Materials and Methods

Chemicals and antibodies

All the chemicals are from Sigma-Aldrich (St. Louis, MO, USA) unless otherwise stated. The affinity purified rabbit polyclonal antibodies to EEA1, ERM, RhoA, Rac2 are from Abcam (Cambridge, England); the purified rat monoclonal anti-LAMP1 is from BD Biosciences (Franklin Lakes, NJ, USA); anti-gp91phox is from Santa Cruz Biotechnology (Santa Cruz, CA, USA); and rabbit polyclonal antiserum to p67phox is a gift from Professor Segal (University College London). Transferrin-FITC is from Auspep (West Melbourne, VIC, Australia). ToPro-3 is from Molecular Probes (Eugene, OR, USA). All the secondary antibodies are made in donkey and are affinity purified and cross species adsorbed (Jackson ImmunoResearch Labs, West Grove, PA, USA).

Animals

All animal work was approved by the Garvan/St Vincent's Hospital animal ethics committee. The germline gene deleted CLIC1$^{-/-}$ mice are on a 129X1/SVJ background and have been previously described (Qiu et al., 2010). In all instances, syngeneic 129X1/SVJ mice or cells derived from them were used as CLIC1$^{+/+}$ control. Gp91phox knock out mice (Dinauer et al., 1997) were kindly provided by Professor Chris Sobey of Monash University, Melbourne, Australia.

Primary murine resident peritoneal cell isolation and macrophage enrichment

Primary murine resident peritoneal cells were harvested using peritoneal lavage (Zhang et al., 2008). RPMI-1640 medium (6 ml) supplemented with FBS (10%), glutamine (2 mM) and 100 U/ml penicillin 100 mg/ml streptomycin was injected into the peritoneal cavity and routinely 5 ml of the medium containing cells was retrieved. The extracted cells were depleted of red blood cells using red blood cell lysis buffer containing 8.3 g/l ammonium chloride in 10 mM Tris-HCl, pH 7.5 and washed by centrifugation. The viable cell number was determined by Trypan Blue exclusion using a Countess Cell Counter (Invitrogen, Grand Island, NY, USA).

The cells harvested were resuspended in the above culture medium then seeded into either 8-well chamber slides (BD Biosciences, Franklin Lakes, NJ, USA) for immunofluorescence microscopy, or in 96 well white walled and clear bottomed plates (Nunc, Rochester, NY, USA) for ROS assay, or onto a Ø42 mm glass coverslip housed in a Petri dish (BD, Franklin Lakes, NJ, USA) for live cell imaging. The peritoneal cells were allowed to adhere for 48 hours after which they were washed three times with culture medium to remove non-adherent cells and to leave the enriched peritoneal macrophages for experimentation.

Opsonisation of zymosan particles

Saccharomyces cerevisiae zymosan A particles were dissolved in PBS and boiled for 30 min before washing and resuspending in PBS (1 mg/ml) for storage at room temperature before use. For opsonisation, the particles were first dispersed by sonication to form a uniform single particle suspension and pelleted by centrifugation, then incubated for 30 min at 37℃ in the serum, which was previously collected and stored in aliquots at −70℃. The opsonised particles were then washed and resuspended in PBS before use.

Synchronised phagocytosis

The cell-containing 8 well chamber slides, tissue culture plates, or coverslips were cooled on ice for 10 min followed by the addition of opsonised zymosan particles. The cells were incubated on ice for a further 20 min to allow the particles to dock to the cells. The slides were then transferred to a 37℃ incubator to allow phagocytosis to proceed for the designated time period. In general, for fluorescence staining or live cell imaging the zymosan particle to cell ratio was regulated to achieve a proportion of 2:1.

Immunofluorescence confocal microscopy

The cells with or without phagocytosed zymosan particles were fixed with 4% paraformaldehyde for 20 min, permeabilised with 0.05% saponin in PBS for 30 min at room temperature and incubated with a blocking buffer containing 2% IgG free BSA (Jackson ImmunoResearch Labs, West Grove, PA, USA) and 5% normal donkey serum (Jackson ImmunoResearch Labs, West Grove, PA, USA) overnight at 4℃. To also inhibit Fc receptor mediated binding of antibodies to cells, the blocking buffer also contained an anti-mouse CD16/CD32, also known as Fcγ III/II receptor (0.5 μg/ml, BD, Franklin Lakes, NJ USA). CLIC1 was stained with an in-house developed affinity purified sheep polyclonal antibody followed by cy3-labelled affinity purified, cross species adsorbed anti-sheep IgG as previously described (Qiu et al., 2010). The cells were then stained with the antibodies against either EEA1, ERM, RhoA, Rac2, p67phox, gp91phox or LAMP1, followed by their respective cy2-labelled secondary antibodies. ToPro-3 was used to identify the nuclei. Confocal images were obtained on a Leica TCS SP confocal microscope and processed using Adobe Photoshop CS2 v.9 software.

Intraphagosomal pH measurement

Intraphagosomal pH was measured using live cell imaging of macrophages which had phagocytosed serum-opsonised zymosan particles covalently linked to a pH sensitive dye: either Oregon Green 488-X (zOG) or FITC (zFITC). To make zOG conjugate, zymosan (5 mg/ml in PBS) was first subject to sonication to form single particle suspension before incubation with Oregon Green 488-X succinimidyl ester (1 mg/ml, Molecular Probes, Eugene, OR, USA) for 2 hours at 37℃. Unbound dye was removed by 10 washes using PBS. zFITC was purchased from Molecular Probes (Eugene, OR, USA). Both labelled zOG and zFITC were stored in PBS (5 mg/ml) supplemented with Na azide (0.01%) at 4℃.

For live cell imaging, macrophages enriched on a Ø42 mm glass coverslip were placed in an incubation chamber containing 2 ml HBSS buffer supplemented with HEPES (10 mM), glucose (6 mM), sodium bicarbonate (10 mM) and sodium pyruvate (1 mM) and mounted onto a heated stage of an inverted Zeiss Axiovert 200 M fluorescence microscope (Carl Zeiss, New York, USA) equipped with a 40×numerical aperture 1.45 objective, a halide light source of Prior Lumen200 and a CCD camera. A neutral density filter was fitted to minimise photobleaching. Over the 30 minutes of recording the loss of fluorescence intensity due to photobleaching is negligible (supplementary material Fig. S1). After initiating synchronised phagocytosis, the fluorescence of either zOGs or zFITCs was recorded over 60 min, in a time-lapse mode, at a rate of one image per minute (excitation 490 nm and emission 525 nm). The brightfield of the same view was also recorded to demonstrate the cell morphology and facilitate the track of phagocytosed zymosan particles.

In some instances, IAA94 (100 μM), a cell permeable CLIC1 ion channel blocker, or DMSO (vehicle) was included in the chamber buffer to test CLIC1 specific effect on phagosomal acidification.

To calibrate the probe fluorescence to phagosomal pH, time lapse recordings were carried out of macrophages that had phagocytosed serum opsonised zOG or zFITC, incubated in a series of buffers from pH 2 to 7.5 which also contained bafilomycin A1 (100 nM), nigericin (10 μM), valinomycin (10 μM) and carbonyl cyanide m-chlorophenylhydrazone (10 μM) to disruption membrane channel activities and allow equilibration of intracellular pH with that of the extracellular buffer. The calibration curves for both zOG and zFITC are shown in supplementary material Fig. S2.

Intraphagosomal proteolysis

Adapting a spectrofluorometric method (Yates and Russell, 2008), we covalently coupled the 3.0 μm carboxylate-modified silica particles (Si-COOH, Kisker Biotech, Steinfurt, Germany) with Alexa Fluor 594(R) carboxylic acid, succinimidyl ester (mixed isomers) (Alexa594-SE) (Molecular Probes, Eugene, OR, USA) and DQ green bodipy BSA (DQ - bodipy BSA, Molecular Probes, Eugene, OR, USA). Live images of intraphagosomal proteolysis of BSA were recorded on a Zeiss Inverted microscope as described above after synchronised phagocytosis of the labelled beads. The fluorescence signals from both the green bodipy (excitation 490, emission 525) and Alexa Fluor 594 (excitation 570, emission 620) were acquired and used for a ratiometric data analysis of intraphagosomal proteolysis.

Live imaging data analysis

Live imagining data analysis was performed using MBF ImageJ64 (NIH). First of all, the brightfield and the fluorescence channels of the images were superimposed to allow tracking phagocytosed beads in the cells. Free unphagocytosed beads are excluded from data analysis. Each phagocytosed bead was followed individually over the observation time and the fluorescence intensity of either the green or the red channel was generated after subtraction of background noise using the intensity vs time plot function of ImageJ64. To avoid bias, all the phagocytosed zymosan particles in the recording optical field were processed for data analysis except for: 1) unhealthy cells which failed to move or change shape over time; or 2) cells that phagocytosed multi-particle zymosan clumps. Typically 5-20% of the cells may be excluded from analysis.

For intraphagosomal pH measurement, the calibration curves were constructed using a non-linear sigmoidal regression in Prism 5 (GraphPad Software Inc., La Jolla, CA, USA) and the conversion of fluorescence intensity to pH was via the built in 'interpolate' read out function.

Generation of Alexa Fluor 488 (AF488)-conjugated experimental particles and measurement of the phagosomal-lysosomal fusion

The experimental AF488-conjugated particles were prepared as previously described (Yates et al., 2005; Yates and Russell, 2008). Approximately 500 μL of 3 μm silica COOH-beads (Kisker Biotech, Steinfurt, Germany) were washed

twice with PBS. The beads were then re-suspended in 1×PBS containing 25 mg/mL of cyanamide and incubated for 15 minutes at room temperature with rotation. Subsequently, the beads were washed in 0.1 M borate buffer (pH 8.0) and re-suspended in borate buffer containing 1 mg of human IgG. The beads were incubated at room temperature for 2-3 minutes, which was followed by addition of 5 mg of fatty acid-free BSA. The beads were then incubated overnight with rotation at 4℃. The following day the beads were washed twice with 0.1 M borate buffer and re-suspended in borate buffer. The bead suspension was then combined with 8 µg of AF488 and incubated at room temperature with rotation for 30 minutes. The beads were then washed twice with 1×PBS containing 100 mM glycine (Sigma, Oakville, ON) to quench any reactive amines. Prior to use the beads were incubated with 10 µg rabbit anti-BSA antibody (Rockland Immunochemicals, Gilbertsville, PA). The beads were used at an MOI of 1-2. The cells were seeded in a microwell plate at confluence in 50 µL of BMMØ growth media containing 50 µg/mL of AF594 hydrazide (Molecular Probes, Carlsbad, CA). The cells were incubated overnight at 37℃ and 7% CO_2. The following day the pulse media containing AF594 was removed and the cells were thoroughly washed with fresh, pre-warmed media. The cells were then chased for 1 hour at 37℃ using fluor-free growth media. The cells were subsequently washed with 100 µL of an assay buffer (1×PBS supplemented with 1 mM $CaCl_2$, 2.7 mM KCl, 0.5 mM $MgCl_2$, 5 mM dextrose, and 0.25% gelatin) followed by addition of the AF488-conjugated beads.

Lysosomal contribution to the phagosome was measured using Förster resonance energy transfer (FRET) efficiency between a particle-conjugated donor fluorophore Alexa Fluor 488 (excitation 485 nm; emmision 520 nm) and a fluid-phase lysosomal acceptor fluorophore Alexa Fluor 594 hydrazide (excitation 594 nm; emmision 615 nm) relative to the donor fluorescence. The changes in fluorescence were recorded using the FLUOstar OPTIMA fluorescent plate reader (BMG Labtech, Ortenberg, Germany) and were reported as relative fluorescent units, which were indicative of the concentration of the lysosomal constituents within the phagosome at any given point in time. Relative fluorescent units (RFU) defined by the equation $RFU=SF_{RT}/CF_{RT}$ (where SF_{RT}=substrate fluorescence in real time and CF_{RT}=calibration fluorescence in real time) were plotted against time. For comparison of phagosomal-lysosomal fusion across experiments, the gradients (as described by the equation $y=mx+c$, where y=RFU, m=gradient, and x=time) of the linear portion of the relative substrate fluorescence plotted against time were calculated.

Microsome preparation

Microsomes were prepared essentially as described (Cox and Emili, 2006). All the procedures were performed on ice. Briefly, BV2 cells maintained in RPMI culture medium were washed then harvested by scraping and the cell pellet resuspended in the homogenisation buffer (HB) containing sucrose (10%) and imidazole (3 mM). dithiothreitol 2 mM was also included in the HB as CLIC1 is sensitive to oxidation. The cytoplasmic membranes were ruptured by passing the cells 15 times through a 25 gauge needle, followed by centrifugation at 1000 g for 15 min at 4℃. The resultant supernatant, or post nuclear supernatant (PNS) which contains a mixture of endosomes and other vesicles are designated here as microsomes. PNS was then subject to ultracentrifugation at 100,000 g for 60 min at 4℃ to separate cytosol fraction and the microsome fraction (pellet).

In vitro BSA proteolysis

Microsomes harvested from ~50,000 cells were resuspended in 20 µl of the lysosome buffer (DTT 2 mM, CHAPS 0.5%, EDTA 0.5 M, Sodium Acetate 100 mM), which had been calibrated to pH 4, 4.2, 4.4 and 4.6 respectively. BSA (100 µg) was added to the 20 µl buffered microsome preparations and incubated for 60 min at 37℃. The proteolytic reactions were terminated when SDS sample buffer (Invitrogen, Grand Island, NY, USA) was added into each vial and heated for 10 min at 70℃. The entire contents were then loaded into a NuPage 4-12% bis-Tris gel (Invitrogen, Grand Island, NY, USA). After electrophoresis at 200 volts for 35 min, the gels were stained with Coomassie Blue R250 and destained. The images were obtained using a ChemiDoc (BioRad, Gladesville, NSW, Australia) with Quantity One software (BioRad, Gladesville, NSW, Australia).

Chemiluminescence measurement of ROS production from peritoneal macrophages

Enriched resident peritoneal macrophages were seeded in a 96 well plate (100,000 cell/well) and cultured for 48 hours before use. For ROS assay, the culture medium was removed and replaced with a reaction mixture containing luminol (50 µM) and horse radish peroxidase (5 units) in 150 µl buffer (in mM: HEPES 10, pH 7.4, NaCl 137, $NaHCO_3$ 12, KCl 2.7, $NaH_2PO_4.2H_2O$ 0.36, glucose 10 and $CaCl_2$ 1). The chemiluminescence intensity from each well was recorded kinetically over 30 min at 37℃ in a microplate reader (FLUOstar OPTIMA, BMG Labtech, Mornington, Vic, Australia). ROS generation in macrophages was stimulated by addition of serum opsonised zymosan (50 µg/ml) at the beginning of the measurement. To compensate for the variation due to uneven seeding of the cells, an accurate determination of the cell number in each well was performed after completion of the experiment using a CyQuant kit (Molecular Probes, Eugene, OR, USA) following manufacturer's instruction and the chemiluminescence signals corrected accordingly.

K/BxN arthritis

K/BxN arthritis was induced in mice by passive serum transfer (Ditzel, 2004). In brief, $CLIC1^{-/-}$ and the age (8-12 weeks) and sex matched $CLIC1^{+/+}$ mice were injected intraperitoneally with a single dose of 300 µl K/BxN serum (Garvan Institute of Medical Research, Darlinghurst, NSW, Australia). The development of arthritis was assessed using a swelling index generated from the thickness of footpads and ankles measured over 28 days using a calliper (Fowler Tools and Instruments, Boston, MA, USA) in millimetre before the injection (baseline) and then once every second day. The swelling index for each time point is calculated as: (thickness/baseline)×100 and plotted over time to compare disease severity.

Statistical data analysis

All data were expressed as the mean±s.e.m. Statistical comparisons were performed using Student's *t*-test or Two-way Repeated-Measures ANOVA as indicated. P values <0.05 were considered to be statistically significant.

Funding

This work was supported by project grants from the Australian National Health and Medical Research Council [grant number 568764] and the University of New South Wales. D.A.B. is an Australian National Health and Medical Research Council Biomedical Career Development Fellow.

Supplementary material available online at
http://jcs.biologists.org/lookup/suppl/doi:10.1242/jcs.110072/-/DC1

References

Barriere, H., Bagdany, M., Bossard, F., Okiyoneda, T., Wojewodka, G., Gruenert, D., Radzioch, D. and Lukacs, G. L. (2009). Revisiting the role of cystic fibrosis transmembrane conductance regulator and counterion permeability in the pH regulation of endocytic organelles. *Mol. Biol. Cell* **20**, 3125-3141.

Berry, K. L., Bülow, H. E., Hall, D. H. and Hobert, O. A. (2003). A *C. elegans* CLIC-like protein required for intracellular tube formation and maintenance. *Science* **302**, 2134-2137.

Bradford, E. M., Miller, M. L., Prasad, V., Nieman, M. L., Gawenis, L. R., Berryman, M., Lorenz, J. N., Tso, P., and Shull, G. E. (2010) CLIC5 mutant mice are resistant to diet-induced obesity and exhibit gastric hemorrhaging and increased susceptibility to torpor. *Am. J. Physiol.* **298**, R1531-1542.

Chalothorn, D., Zhang, H., Smith, J. E., Edwards, J. C. and Faber, J. E. (2009). Chloride intracellular channel-4 is a determinant of native collateral formation in skeletal muscle and brain. *Circ. Res.* **105**, 89-98.

Cox, B. and Emili, A. (2006). Tissue subcellular fractionation and protein extraction for use in mass-spectrometry-based proteomics. *Nat. Protoc.* **1**, 1872-1878.

DeCoursey, T. E. (2010). Voltage-gated proton channels find their dream job managing the respiratory burst in phagocytes. *Physiology (Bethesda)* **25**, 27-40.

Deriy, L. V., Gomez, E. A., Zhang, G., Beacham, D. W., Hopson, J. A., Gallan, A. J., Shevchenko, P. D., Bindokas, V. P. and Nelson, D. J. (2009). Disease-causing mutations in the cystic fibrosis transmembrane conductance regulator determine the functional responses of alveolar macrophages. *J. Biol. Chem.* **284**, 35926-35938.

Di, A., Brown, M. E., Deriy, L. V., Li, C., Szeto, F. L., Chen, Y., Huang, P., Tong, J., Naren, A. P., Bindokas, V. et al. (2006). CFTR regulates phagosome acidification in macrophages and alters bactericidal activity. *Nat. Cell Biol.* **8**, 933-944.

Dinauer, M. C., Deck, M. B. and Unanue, E. R. (1997). Mice lacking reduced nicotinamide adenine dinucleotide phosphate oxidase activity show increased susceptibility to early infection with Listeria monocytogenes. *J. Immunol.* **158**, 5581-5583.

Ditzel, H. J. (2004). The K/BxN mouse: a model of human inflammatory arthritis. *Trends Mol. Med.* **10**, 40-45.

Erwig, L.-P., McPhilips, K. A., Wynes, M. W., Ivetic, A., Ridley, A. J. and Henson, P. M. (2006). Differential regulation of phagosome maturation in macrophages and dendritic cells mediated by Rho GTPases and ezrin-radixin-moesin (ERM) proteins. *Proc. Natl. Acad. Sci. USA* **103**, 12825-12830.

Gagnon, L. H., Longo-Guess, C. M., Berryman, M., Shin, J. B., Saylor, K. W., Yu, H., Gillespie, P. G. and Johnson, K. R. (2006). The chloride intracellular channel protein CLIC5 is expressed at high levels in hair cell stereocilia and is essential for normal inner ear function. *J. Neurosci.* **26**, 10188-10198.

Haggie, P. M. and Verkman, A. S. (2007). Cystic fibrosis transmembrane conductance regulator-independent phagosomal acidification in macrophages. *J. Biol. Chem.* **282**, 31422-31428.

Hara-Chikuma, M., Yang, B., Sonawane, N. D., Sasaki, S., Uchida, S. and Verkman, A. S. (2005). ClC-$_3$ chloride channels facilitate endosomal acidification and chloride accumulation. *J. Biol. Chem.* **280**, 1241-1247.

Harrop, S. J., DeMaere, M. Z., Fairlie, W. D., Reztsova, T., Valenzuela, S. M., Mazzanti, M., Tonini, R., Qiu, M. R., Jankova, L., Warton, K. et al. (2001).

Crystal structure of a soluble form of the intracellular chloride ion channel $CLIC_1$ (NCC_{27}) at 1.4-Å resolution. *J. Biol. Chem.* **276**, 44993-45000.

He, G., Ma, Y., Chou, S.-Y., Li, H., Yang, C., Chuang, J.-Z., Sung, C.-H. and Ding, A. (2011). Role of CLIC4 in the host innate responses to bacterial lipopolysaccharide. *Eur. J. Immunol.* **41**, 1221-1230.

Kannan, K., Ortmann, R. A. and Kimpel, D. (2005). Animal models of rheumatoid arthritis and their relevance to human disease. *Pathophysiology* **12**, 167-181.

Lamb, F. S., Moreland, J. G. and Miller, F. J., Jr (2009). Electrophysiology of reactive oxygen production in signaling endosomes. *Antioxid. Redox Signal.* **11**, 1335-1347.

Landry, D. W., Akabas, M. H., Redhead, C., Edelman, A., Cragoe, E. J., Jr and Al-Awqati, Q. (1989). Purification and reconstitution of chloride channels from kidney and trachea. *Science* **244**, 1469-1472.

Littler, D. R., Harrop, S. J., Goodchild, S. C., Phang, J. M., Mynott, A. V., Jiang, L., Valenzuela, S. M., Mazzanti, M., Brown, L. J., Breit, S. N. et al. (2010). The enigma of the CLIC proteins: ion channels, redox proteins, enzymes, scaffolding proteins? *FEBS Lett.* **584**, 2093-2101.

Liu, K.-J. and Chu, C.-L. (2006). Current progress in dendritic cell research. *J. Cancer Mol.* **2**, 217-220.

Lukacs, G. L., Rotstein, O. D. and Grinstein, S. (1990). Phagosomal acidification is mediated by a vacuolar-type H^+-ATPase in murine macrophages. *J. Biol. Chem.* **265**, 21099-21107.

Marion, S., Hoffmann, E., Holzer, D., Le Clainche, C., Martin, M., Sachse, M., Ganeva, I., Mangeat, P. and Griffiths, G. (2011). Ezrin promotes actin assembly at the phagosome membrane and regulates phago-lysosomal fusion. *Traffic* **12**, 421-437.

Okochi, Y., Sasaki, M., Iwasaki, H. and Okamura, Y. (2009). Voltage-gated proton channel is expressed on phagosomes. *Biochem. Biophys. Res. Commun.* **382**, 274-279.

Pierchala, B. A., Muñoz, M. R. and Tsui, C. C. (2010). Proteomic analysis of the slit diaphragm complex: CLIC5 is a protein critical for podocyte morphology and function. *Kidney Int.* **78**, 868-882.

Qiu, M. R., Jiang, L., Matthaei, K. I., Schoenwaelder, S. M., Kuffner, T., Mangin, P., Joseph, J. E., Low, J., Connor, D., Valenzuela, S. M. et al. (2010). Generation and characterization of mice with null mutation of the chloride intracellular channel 1 gene. *Genesis* **48**, 127-136.

Russell, D. G., Vanderven, B. C., Glennie, S., Mwandumba, H. and Heyderman, R. S. (2009). The macrophage marches on its phagosome: dynamic assays of phagosome function. *Nat. Rev. Immunol.* **9**, 594-600.

Rybicka, J. M., Balce, D. R., Khan, M. F., Krohn, R. M. and Yates, R. M. (2010). NADPH oxidase activity controls phagosomal proteolysis in macrophages through modulation of the lumenal redox environment of phagosomes. *Proc. Natl. Acad. Sci. USA* **107**, 10496-10501.

Rybicka, J. M., Balce, D. R., Chaudhuri, S., Allan, E. R. and Yates, R. M. (2011). Phagosomal proteolysis in dendritic cells is modulated by NADPH oxidase in a pH-independent manner. *EMBO J.* **31**, 932-944.

Scott, C. C. and Gruenberg, J. (2011). Ion flux and the function of endosomes and lysosomes: pH is just the start: the flux of ions across endosomal membranes influences endosome function not only through regulation of the luminal pH. *Bioessays* **33**, 103-110.

Seetoo, K. F., Schonhorn, J. E., Gewirtz, A. T., Zhou, M. J., McMenamin, M. E., Delva, L. and Simons, E. R. (1997). A cytosolic calcium transient is not necessary for degranulation or oxidative burst in immune complex-stimulated neutrophils. *J. Leukoc. Biol.* **62**, 329-340.

Segal, A. W. and Shatwell, K. P. (1997). The NADPH oxidase of phagocytic leukocytes. *Ann. N. Y. Acad. Sci.* **832**, 215-222.

Singh, A. K., Afink, G. B., Venglarik, C. J., Wang, R. P. and Bridges, R. J. (1991). Colonic Cl channel blockade by three classes of compounds. *Am. J. Physiol.* **261**, C51-C63.

Solomon, S., Rajasekaran, N., Jeisy-Walder, E., Snapper, S. B. and Illges, H. (2005). A crucial role for macrophages in the pathology of K/B × N serum-induced arthritis. *Eur. J. Immunol.* **35**, 3064-3073.

Steinberg, B. E., Huynh, K. K., Brodovitch, A., Jabs, S., Stauber, T., Jentsch, T. J. and Grinstein, S. (2010). A cation counterflux supports lysosomal acidification. *J. Cell Biol.* **189**, 1171-1186.

Sun-Wada, G. H., Tabata, H., Kawamura, N., Aoyama, M. and Wada, Y. (2009). Direct recruitment of H^+-ATPase from lysosomes for phagosomal acidification. *J. Cell Sci.* **122**, 2504-2513.

Tonini, R., Ferroni, A., Valenzuela, S., Warton, K., Campbell, T. J., Breit, S. N. and Mazzanti, M. (2000) Characterisation of the NCC27 nuclear chloride ion channel: Comparison of its electrophysiological properties on the nuclear and plasma membranes and inhibition of its conductance in transfected CHO-K1 cells by antibody blockade. *FASEB J.* **14**, 1171-1178.

Tulk, B. M., Schlesinger, P. H., Kapadia, S. A., and Edwards, J. C. (2000) CLIC1 functions as a chloride channel when expressed and purified from bacteria. *J. Biol. Chem.* **275**, 26986-26993.

Tulk, B. M., Kapadia, S. and Edwards, J. C. (2002). CLIC1 inserts from the aqueous phase into phospholipid membranes, where it functions as an anion channel. *Am. J. Physiol. Cell Physiol.* **282**, C1103-C1112.

Ulmasov, B., Bruno, J., Gordon, N., Hartnett, M. E. and Edwards, J. C. (2009). Chloride intracellular channel protein-4 functions in angiogenesis by supporting acidification of vacuoles along the intracellular tubulogenic pathway. *Am. J. Pathol.* **174**, 1084-1096.

Valenzuela, S. M., Martin, D. K., Por, S. B., Robbins, J. M., Warton, K., Bootcov, M. R., Schofield, P. R., Campbell, T. J. and Breit, S. N. (1997). Molecular cloning and expression of a chloride ion channel of cell nuclei. *J. Biol. Chem.* **272**, 12575-12582.

van Fürden, D., Johnson, K., Segbert, C. and Bossinger, O. (2004). The *C. elegans* ezrin-radixin-moesin protein ERM-1 is necessary for apical junction remodelling and tubulogenesis in the intestine. *Dev. Biol.* **272**, 262-276.

Vieira, O. V., Botelho, R. J. and Grinstein, S. (2002). Phagosome maturation: aging gracefully. *Biochem. J.* **366**, 689-704.

Warton, K., Tonini, R., Fairlie, W. D., Matthews, J. M., Valenzuela, S. M., Qiu, M. R., Wu, W. M., Pankhurst, S., Bauskin, A. R., Harrop, S. J. et al. (2002). Recombinant $CLIC_1$ (NCC_{27}) assembles in lipid bilayers via a pH-dependent two-state process to form chloride ion channels with identical characteristics to those observed in Chinese hamster ovary cells expressing $CLIC_1$. *J. Biol. Chem.* **277**, 26003-26011.

Yates, R. M. and Russell, D. G. (2008). Real-time spectrofluorometric assays for the lumenal environment of the maturing phagosome. *Methods Mol. Biol.* **445**, 311-325.

Yates, R. M., Hermetter, A. and Russell, D. G. (2005). The kinetics of phagosome maturation as a function of phagosome/lysosome fusion and acquisition of hydrolytic activity. *Traffic* **6**, 413-420.

Zhang, X., Goncalves, R. and Mosser, D. M. (2008). The isolation and characterisation of murine macrophages. *Curr. Prot. Immunol.* 14.1.1-14.1.14.

Log in to My Ulrich's

Macquarie University Library --Select Language--

Search Workspace Ulrich's Update Admin

Enter a Title, ISSN, or search term to find journals or other periodicals:

0021-9533

Advanced Search

Search My Library's Catalog: ISSN Search | Title Search

Search Results

Journal of Cell Science

Title Details | Table of Contents

Related Titles

- Alternative Media Edition (2)
- Supplement (1)

Lists

Marked Titles (0)

Search History

0021-9533 - (1)

Save to List Email Download Print Corrections Expand All Collapse All

Basic Description

Title	Journal of Cell Science
ISSN	0021-9533
Publisher	The Company of Biologists Ltd.
Country	United Kingdom
Status	Active
Start Year	1852
Frequency	Semi-monthly
Volume Ends	Dec
Language of Text	Text in: English
Refereed	Yes
Abstracted / Indexed	Yes
Serial Type	Journal
Content Type	Academic / Scholarly
Format	Print
Website	http://jcs.biologists.org
Description	Covers all aspects of cell biology. Of interest to cell biologists, molecular biologists, geneticists, and particularly those working in the cell cycle and cell signaling fields.

- Subject Classifications
- Additional Title Details
- Title History Details
- Publisher & Ordering Details
- Price Data
- Online Availability
- Abstracting & Indexing
- Other Availability
- Demographics
- Reviews

Save to List Email Download Print Corrections Expand All Collapse All